

## **Preliminary design review (PDR)**

---

# **Package Delivery Aircraft (Jark MK.II)**

---

Presented to the  
University of California, San Diego  
Department of Mechanical and Aerospace Engineering

MAE 155B

April 30th, 2025

Prepared by:

---

**Team 3 MJ<sup>5</sup>**

---

Jeffrey Denenberg, Jeffrey Bratman, Johnpierre Khachi,  
Mark Gabriel Samac, Justin Rector, Joseph Tuazon

# Table of Contents

<b>Table of Contents.....</b>	<b>2</b>
<b>Figures &amp; Tables.....</b>	<b>3</b>
<b>Nomenclature.....</b>	<b>5</b>
<b>1. Executive Summary.....</b>	<b>7</b>
<b>2. Introduction.....</b>	<b>9</b>
<b>3. Concept of Operations.....</b>	<b>9</b>
3.1 Requirements and Constraints.....	9
3.2 Operations and Mission Profile.....	9
<b>4. Sizing Analysis.....</b>	<b>10</b>
4.1 Scoring Function.....	10
<b>5. Configuration and Design.....</b>	<b>11</b>
5.1 Wing Design.....	11
5.2 Fuselage Structure.....	12
5.3 Landing Gear Choice.....	13
5.4 Package Drop-off Mechanism.....	13
<b>6. Aerodynamics.....</b>	<b>14</b>
6.1 Assumptions.....	14
6.2 Airfoil Selection.....	14
6.3 Drag Buildup.....	15
<b>7. Performance.....</b>	<b>16</b>
7.1 Takeoff.....	16
7.2 Cruise.....	16
7.3 Maneuvering and Climb.....	17
<b>8. Propulsion.....</b>	<b>18</b>
8.1 Propulsion System Design.....	18
<b>9. Weights and Balances.....</b>	<b>18</b>
9.1 Weight Breakdown.....	18
9.2 Tail Sizing.....	19
9.3 Stability.....	19
<b>10. Conclusion.....</b>	<b>20</b>
<b>References.....</b>	<b>21</b>
<b>Appendices.....</b>	<b>22</b>
Appendix A - Figures.....	22
Appendix B - Equations.....	29
Appendix C - Tables.....	32

# Figures & Tables

Table 1.1: Aircraft Requirements and Specifications supervised in MAE 155B Course.....	7
Figure 1.2: Cross sectional view of the aircraft.....	8
Table 2.2: Measures of Merit.....	9
Table 3.1: Targets and Constraints for a radio-powered aircraft.....	9
Table 3.2: The two missions of the aircraft and corresponding descriptions.....	10
Table 4.1: The J gain [\\$] per unit increase of a payload parameter, while keeping the other fixed.....	11
Figure 5.1: The skeletal wing structure design with wooden rib and spars, along with aileron.....	12
Figure 5.2: The CAD skeletal structure of the aircraft fuselage.....	12
Figure 5.3: The two proposed mechanisms for two-door opening and closing, gear-driven (left) and lever (right).....	13
Table 6.1: Main wing dimensions.....	14
Figure 6.1: Selected Airfoils 2-D Aerodynamic Analysis at $Re = 500,000$ and cruise speed of 25 m/s. Data imported from XFOIL. Lift Coefficient (top) and Drag Coefficient (bottom) vs Angle of Attack. Stall Angle of Attack at $13.25^\circ$ .....	15
Table 6.2: Major Aerodynamic Parameters of selected airfoil, NACA 4412.....	15
Figure 6.2: 2-D and 3-D comparison. Lift coefficient with $CL_{max}$ at $13.25^\circ$ stall angle of attack (top); Drag coefficient vs angle of attack, 3-D includes the drag build-up for wing, fuselage, tails, propeller and landing gear. (bottom).....	16
Figure 7.1: Thrust required for steady level flight given different cruise velocities.....	17
Figure 7.2: T/W vs Wing loading at set performance and aerodynamic design parameters.....	17
Table 8.1: Propulsion Key Parameters comparison between 9x6E and 8x6E.....	18
Figure 9.1: Breakdown of Aircraft Weight and Material Composition.....	19
Table 9.1: Tail Sizing Dimensions.....	19
Table 9.2: Aerodynamic stability results.....	20
Figure A.5.1: The landing gear configuration (Tail dragger).....	22
Figure A.6.1: K" estimation from the 2-D aerodynamic data for 3-D aerodynamic data calculations in Figure 6.2.....	23
Figure A.6.2: Other 2-D aerodynamic data for selected airfoils at $Re = 500,000$ . Data collected from XFOIL.....	23
Figure A.7.1: The Graphical User Interface (GUI) of takeoff distance and stall speed calculations using MATLAB.....	24
Figure A.7.2: Top View of Mission Bay Runway with approximate total runway distance (80m) using ArduPilot Mission Planner Software.....	24
Figure A.8.1: Efficiency of different propellers as a function of advance ratio.....	25
Figure A.8.1: Power coefficient of different propellers as a function of advance ratio.....	25
Figure A.8.2: Torque coefficient of different propellers as a function of advance ratio.....	26
Figure A.8.3: Thrust coefficient of different propellers as a function of advance ratio.....	26
Figure A.9.1: Image of table 6.4 from Raymer [1] textbook that lists typical Tail Volume Coefficients. 27	
Figure A.9.2: Plots of different dd vs r coefficient at varying taper, m coefficient, and aspect ratio..	28
B.4.1: Gross Weight Equation:.....	29

B.4.2: Scoring Function Equation.....	29
B.6.1: Total Drag Coefficient Equation.....	29
B.6.2: Drag Buildup — form and interference drag Equation.....	29
B.6.3: Reynolds Number Equation.....	29
B.6.4: 3-D Maximum Lift Coefficient Equation.....	29
B.7.1-4: Aircraft Takeoff Distance Equations.....	30
B.7.5-6: Climb and Maneuvering Thrust to Weight Equations.....	30
B.8.2: Elevon Area Equation.....	30
B.9.1: Horizontal and Vertical Tail Planform Area Equation.....	30
B.9.2: Center of Gravity Location Equation.....	30
B.9.3: Horizontal Tail Lift Curve slope Equation.....	31
B.9.4: Neutral Point Location formula.....	31
B.9.5: Static Margin Equation.....	31
Table C.4.1: Scoring Function's fixed parameter values.....	32
Table C.4.2: Scoring Function's Parameter Assumptions and Values.....	32
Table C.4.3: Assumptions on initial gross weight and wing area based on student-built aircrafts (MAE 155B).....	32
Table C.5.1: List of the fixed components and available components.....	33
Table C.5.2: List of the available parts and materials.....	33
Table C.5.3: List of the other available parts and materials.....	34
Table C.5.4: List of the propeller choices.....	34
Table C.6.1: Drag buildup for the 3D drag aerodynamic analysis.....	34
Table C.8.1: Specifications of the required brushless motor.....	35
Table C.8.2: Specifications of the required battery.....	35
Table C.8.3: List of the fixed components and available components.....	36
Table C.8.4: List of the propeller size choices and corresponding RPMs.....	36
Table C.9.1: List of individual component's mass and center of gravity location from fuselage structure nose along X axis; electronics box includes battery, receiver, ESC, Watt meter and balsa wood structure.....	37
Table C.9.2: Aerodynamic parameters used to calculate Neutral point.....	37
Table C.9.3: List of various off shelf propellers for Cobra C2217 motor at set 11.1 input voltage. [5]...	
	38

## Nomenclature

$x$	Aircraft design	$W_g$	Gross weight
$W_p(x)$	Payload 1 weight (high weight)	$W_p$	Payload weight
$V_p(x)$	Package 2 volume (high volume)	$W_e$	Empty weight
$E_f(x)$	Energy consumption	$W_s$	Energy-storage weight (batteries)
$W_g(x)$	Gross weight	$W_f$	Fuel weight
$T_f(x)$	Flight time	$W_b$	Battery weight
$r_{wp}$	Revenue per unit weight	$V_p$	Payload volume
$r_{vp}$	Revenue per unit volume	$R$	Range
$c_e$	Cost per unit energy	$\eta_b$	Conversion efficiency (battery to thrust power)
$c_c$	Cost per flight	$e_b$	Battery specific energy (energy per unit mass)
$c_{Wg}$	Cost per unit gross weight	$g$	Acceleration due to gravity
$c_f$	Fixed operating cost	$\frac{L}{D}$	Lift-to-drag ratio in cruise
$t_{;}$	Total aircraft-lift flight time	$D$	Propeller diameter
$C_{l,max}$	2D maximum lift coefficient	$R$	Propeller radius
$C_{Lmax}$	3D max $c_L \doteq 0.9C_{l,max} \cos\Lambda$	$c$	Chord (radial distribution)
$C_d$	2D drag coefficient	$\beta$	Pitch or twist (radial distribution)
$C_D$	3D drag coefficient	$\omega$	Angular speed (rad/s)
$C_{D,0}$	Parasite drag coefficient at zero lift	$n$	Rotational speed (rev/s)
$S$	Wing area	$V_\infty$	Inflow velocity

$AR$	Aspect ratio	$C_T$	Thrust coefficient := $\frac{T}{\rho n^2 D^4}$
$\Lambda$	Wing sweep (quarter-chord line)	$C_Q$	Torque coefficient := $\frac{Q}{\rho n^2 D^5}$
$\lambda$	Taper ratio := $\frac{c_{tip}}{c_{root}}$	$C_P$	Power coefficient := $\frac{P}{\rho n^3 D^5}$
$t/c$	Thickness-to-chord ratio	$J$	Advance ratio := $\frac{V}{nD}$
$\gamma$	Dihedral	$\eta$	Efficiency := $\frac{TV_\infty}{Q\omega}$
Re	Reynold's number	$S$	Disk area := $\pi R^2$
$p$	Air Pressure	$T/S$	Disk loading
T	Air Temperature	$FOM$	Figure of merit := $\frac{T}{P} \sqrt{\frac{T}{2\pi R^2 \rho}}$
$\rho$	Air density	$d_{forward}$	horizontal distance from the CG's vertical line to the main wheels
$q$	Dynamic pressure	$h_{CG}$	height of the CG above the ground
$e$	Oswald efficiency factor	$\theta$	Target angle
$\mu$	Dynamic viscosity		
$C_{d,min}$	2D minimum drag coefficient		
$C_{l,min}$	2D minimum lift coefficient		
$\alpha_0$	Angle-of-attack at $C_l = 0$		

# 1. Executive Summary

The objective of this design project is to develop a remote-controlled (RC) delivery aircraft capable of simulating multi-package delivery missions, with an emphasis on maximizing profit per flight. The aircraft is required to carry two distinct package types: Package 1, a weight-based package with a minimum mass of 0.5 lb, and Package 2, a volume-based package with a minimum volume of 500 cm<sup>3</sup>.

Utilizing a predefined scoring function *Appendix B.4.2*, various mission configurations were evaluated to determine the most profitable delivery strategy. Analysis revealed that prioritizing the delivery of the weight-based package consistently yielded higher returns when the volume-based payload was held at its minimum. This finding directly shaped the aircraft's sizing and configuration.

Initial sizing was informed by historical student aircraft data, targeting a cruise speed of  $\sim 20$  m/s, wing loading of  $\sim 2$  lb/ft<sup>2</sup>, and a thrust-to-weight ratio of  $\sim 0.8$ , resulting in a gross weight of  $\sim 2$  kg and a wing area of  $\sim 0.27$  m<sup>2</sup>. A high-wing design with a 3° dihedral was chosen to improve roll stability, and the wing will be constructed using a lightweight balsa rib-and-spar structure to minimize weight and simplify fabrication. The semi-monocoque plywood fuselage will be optimized for internal payload capacity, with planned material cutouts to reduce structural weight by approximately 200g. A taildragger landing gear configuration will be implemented to improve takeoff performance and provide additional ground clearance. To enable mid-flight delivery of Package 2, two servo-actuated hatch door mechanisms are being developed and will be tested for clean and reliable deployment. Together, these planned design choices form a cohesive strategy that balance aerodynamic efficiency, structural integrity, and mission-specific functionality. Aiming to deliver a profit-optimized aircraft tailored for dual-payload delivery missions.

**Table 1.1:** Aircraft Requirements and Specifications supervised in MAE 155B Course.

<b>MAIN AIRCRAFT SPECIFICATIONS</b>		<b>FLIGHT REQUIREMENTS</b>
<b>Empty Weight</b>	2.9 [lb]	1 The payload packages must consist of lead weights [P1] and an empty cube cardboard box [P2].
<b>Gross Weight</b>	4.4 [lb]	2 The payload weight must be <b>at least 0.5 lbs</b> [P1] and volume <b>at least 500 cm<sup>3</sup></b> [P2].
<b>Payload Weight</b>	1.5 [lb]	3 Mission Bay Park atmospheric condition parameters: pressure, $p$ , of <b>101.28 kPa</b> , temperature, $T$ , of <b>286 K</b> , density, $\rho$ , of <b>1.23 kg/m<sup>3</sup></b> , and dynamic viscosity, $\mu$ , of <b><math>1.80 \times 10^{-5}</math> Pa·s</b>
<b>Payload Hold Volume</b>	64 in <sup>3</sup>	
<b>Empty Weight Fraction</b>	0.66	4 Flight Area Range minimum of <b>600 m</b>
<b>Wingspan</b>	3.77 [ft]	
<b>Aspect Ratio</b>	6.75	
<b>Wing Loading</b>	2.09 [lb/ft <sup>2</sup> ]	
<b>Thrust-to-Weight</b>	0.5	
<b>Cruise Speed</b>	65.62 [ft/s]	

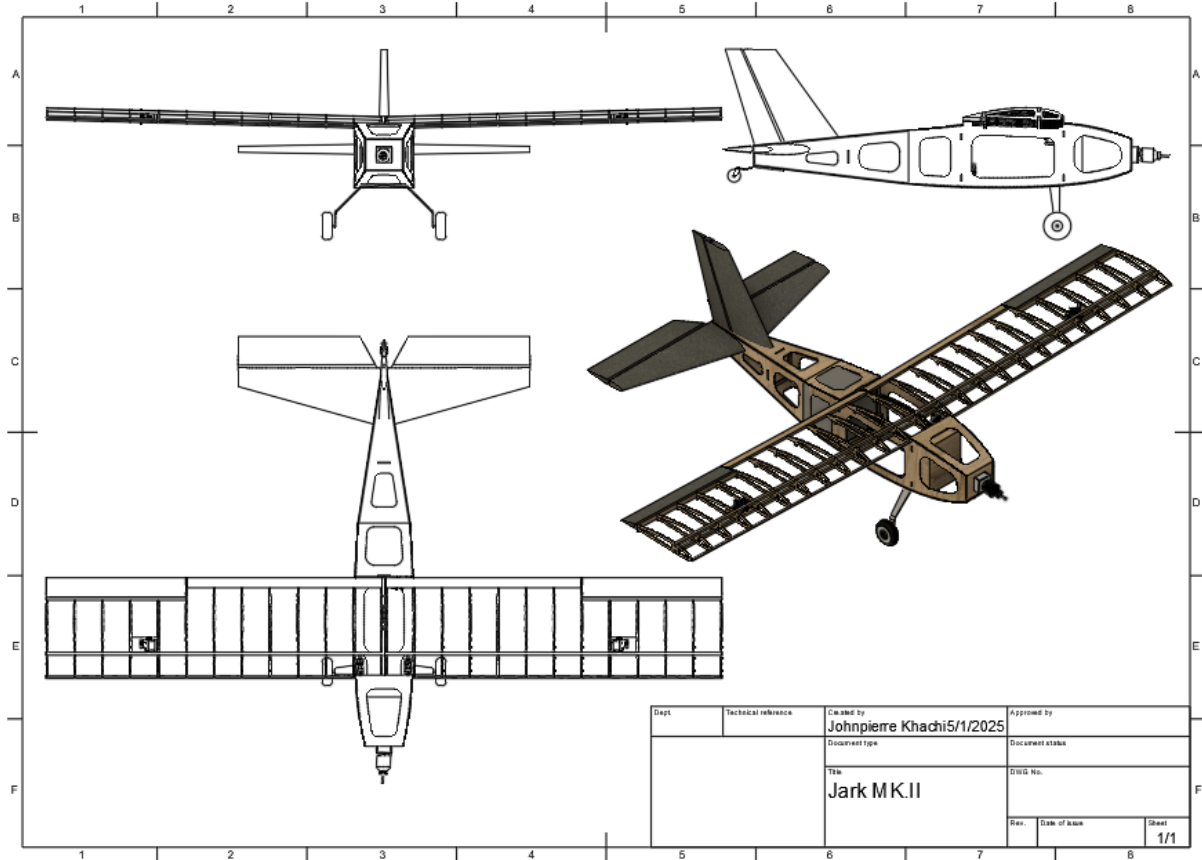


**Figure 1.1:** Isometric and 3-view of the aircraft.

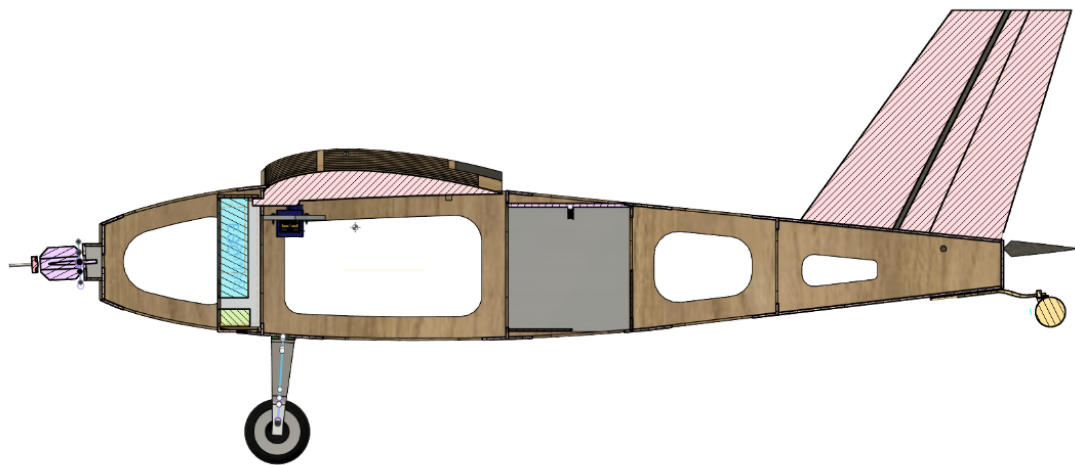


**Figure 1.2:** Cross sectional view of the aircraft.

## 2. Introduction

In our post-pandemic world, e-commerce giants like Amazon, Doordash, and Walmart are rapidly expanding their reach to provide fast, reliable, and sustainable delivery services. Unmanned aerial systems, such as RC planes can fill the niche of fast delivery with minimal environmental impact. Such capability is especially valuable during certain situations such as delivery of medical equipment in remote locations and rapid deployment of critical components. The RC plane proposed is designed to accommodate two distinct payload configurations: high weight with low volume [P1], and high volume with low weight [P2].

CATEGORY	ASPECT
Financial	<ul style="list-style-type: none"> <li>\$720 total budget allotted</li> </ul>
Mission & Maintainability	<ul style="list-style-type: none"> <li>Our goal is to carry two packages, a high-weight and a high-volume; only dropping off the latter</li> </ul>
Environmental Factors	<ul style="list-style-type: none"> <li>Zero emissions and low noise from a battery-powered propeller</li> </ul>
Structures & Weights	<ul style="list-style-type: none"> <li>Structural integrity is maintained by utilizing low-weight balsa wood frames and carbon fiber spars</li> </ul>

Table 2.2: Measures of Merit

## 3. Concept of Operations

### 3.1 Requirements and Constraints

REQUIREMENTS	CONSTRAINTS
<b>Airframe:</b> wing, fuselage, horizontal tail, vertical tail, landing gear	<b>Motor:</b> Cobra C-2217/16 Brushless, Kv=1180
<b>Propulsion system:</b> propeller, motor, speed controller, battery, (battery charger)	<b>Speed controller:</b> Flite Test 40 Amp ESC
<b>Radio control:</b> receiver, (transmitter, transmitter battery)	<b>Battery:</b> Tattu 11.1V 1800mAh 3S 45C LiPo
<b>Actuation:</b> control surfaces, servos, servo push rods, control horns, servo extensions	<b>Receiver:</b> FrSky Taranis Receiver X8R 8 Channel 2.4 GHz
<b>Easily Accessible:</b> easily removable watt meter and battery	<b>ESC:</b> Powerwerx Watt Meter-Bare, DC Inline Power Analyzer, 45A Continuous

Table 3.1: Targets and Constraints for a radio-powered aircraft

### 3.2 Operations and Mission Profile

All aircrafts are expected to perform a ground roll test for the aircraft's yaw control from the contact between the flight area's dirt field and the landing gear. This test allows the pilots to familiarize themselves in landing the aircraft. There are two primary flight missions to be

performed. In *Table 3.2*, a successful empty payload flight allows the team to perform the payload flight. The payload flight demands to carry both payloads, the weight-based [P1] and volume-based payload [P2], and to eject only the volume-based payload midair at a designated point. Although the aircraft's glide ability is imperative, it is expected that it can survive multiple crashes and be repaired easily.

MISSION #	PAYOUT	DETAILS
1	Empty	Perform a successful flight without payload to participate in the competition, required to perform the next mission
2	Weight-Based [P1] & Volume-Based [P2]	Carry a package consisting of lead weights, with a minimum weight of 0.5 lbs and eject an empty cubical box mid-air, with a minimum volume of 500 cm <sup>3</sup> ;

**Table 3.2:** The two missions of the aircraft and corresponding descriptions.

## 4. Sizing Analysis

### 4.1 Scoring Function

To evaluate the effectiveness and overall performance of our aircraft design, we were given a scoring function that incorporates payload delivery capabilities, energy efficiency, flight duration, and other operational cost parameters. Our goal was to maximize our performance by finding the highest score we can get using the function *Appendix B.4.2*. The fixed operational cost parameters are provided in *Appendix C.4.1*. Since the values are fixed and constant, the scoring function can be simplified and weighed by the aircraft overall weight  $Wg(x)$ , payload weight  $Wp(x)$ , payload volume  $Vp(x)$ , battery energy consumption  $Ef(x)$  and the overall flight time  $Tf(x)$ . Changing the values of these parameters yield both gains and trade-offs. The simplified scoring function will guide us in designing our aircraft.

Using the scoring framework, we simplified the aircraft's battery consumption  $Ef(x)$  as it depends on the thrust required to maintain cruise and power input, which can further be reduced to a function that depends on our assumed lift-to-drag ratio  $L/D$  and cruise speed. Our energy source, an 11.1V 1.8Ah battery, was estimated to provide 453,070 J/kg and was assumed to have an efficiency of 85%. The other assumptions are given in *Appendix C.4.2*. We are able to conclude that the cost of increasing the energy consumption is negligible through  $Ef(x)$ 's low quantitative value. Like the energy consumption, the overall flight time heavily depends on cruise speed in which we don't have liberty to control as the aircraft is powered by one motor. We acknowledge that our scoring function will ignore the effects of  $Ef(x)$  and  $Tf(x)$ .

In the end, our team decided that one of the goals of the scoring function analysis was to find the right payload volume to design our fuselage around. With this, we compromised on increasing the payload volume from minimum up to a volume of 64 in<sup>3</sup>. We will be designing a

fuselage that can accommodate this cubic volume. We concluded that the scoring function will only be a stepping stone to start our aircraft design. Another goal was to compromise on a starting payload weight, a minor constraint for us, such that we can increase it depending on the future aircraft performance results. We are only physically capable of increasing the payload weight with a  $J$  gain [\\$] of 7.5 \\$ per unit weight *Table 4.1*, mainly because the payload weight will strategically be placed around the center of gravity (CG). Steadily increasing its value will have more benefits than increasing the payload volume. For now, our payload weight is compromised to be 1.5 lb and will be subjected for changes.

	ASSUMPTION	VALUE
$J$ [\\$] gained per unit payload weight, $W_p$	fixed $V_p$ of 500 cm <sup>3</sup>	7.50 \\$/lb
$J$ [\\$] gained per unit payload volume, $V_p$	fixed $W_p$ of 0.5 lb	2.25 \\$/cm <sup>3</sup>

**Table 4.1:** The  $J$  gain [\\$] per unit increase of a payload parameter, while keeping the other fixed

## 5. Configuration and Design

The aircraft development heavily focuses on meeting the operational requirements, which corresponds to the minimum payload weight and volume. The scoring function analysis has provided the additional weight we can add into the aircraft, specifically how much payload weight until the drawbacks outweigh the score increase. The aforementioned analysis also revealed the limited volume range of the cubical box payload. The fuselage design will prioritize maintaining structural integrity while also accommodating an assumed 64 in<sup>3</sup> cardboard box and other components. The wing will be designed based on an airfoil that maximizes lift best among selected airfoils. Its dimensions are calibrated to provide substantial lift for the aircraft, and its skeletal structure will be optimized for weight and overall wing structural integrity. A taildragger landing gear configuration was decided in order to improve the aircraft's takeoff and landing performance due to the additional angle-of-attack for the wing. Another reason is to minimize the possible interference of the package drop-off mechanism with the landing gears. Lastly, a cargo door mechanism will be adopted to drop the package mid-air. It will undergo several adjustments to incorporate reliability during unloading, straightforwardness, and practicality in terms of maintenance. Together, these elements will form a cohesive design that balances performance, functionality, and manufacturability. Component details are in *Appendix C.5*.

### 5.1 Wing Design

In terms of wing structure construction, we adopted a rib-and-spar configuration made with balsa wood. Balsa offers an excellent balance between strength and weight, which allows us to keep the structure lightweight and still obtain sufficient stiffness to handle aerodynamic wing loads. The use of balsa wood ribs allows an easier manufacturing process and modification when it comes to design refinements. The aforementioned refinement pertains to keeping the aircraft

lightweight and structurally durable. Compared to using foams, this approach has room to improve the wing's overall performance and also emphasizes adaptability to future revisions.

A high-wing configuration was selected with a positive dihedral angle of  $3^\circ$  to enhance flight stability, particularly along the roll axis. This allows an improvement to the aircraft's ability to self-correct after a disturbance, events when the aircraft banks due to a gust or a maneuver. The dihedral effect produces a restoring moment that aids the aircraft to return to level flight without excessive pilot or autopilot input. This configuration is especially useful for maintaining consistent and stable flight during package transport missions.

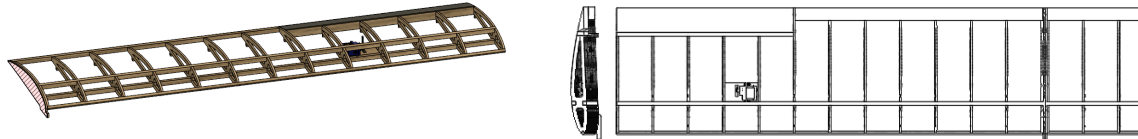


**Figure 5.1:** The skeletal wing structure design with wooden rib and spars, along with aileron.

## 5.2 Fuselage Structure

A simple box-shaped design built from lightweight plywood was adopted for the fuselage. As mentioned in previous configuration justifications, manufacturing should be easy to execute while also keeping structural integrity in mind. An initial box form fuselage naturally provides the best room to house the packages and critical onboard components without complicated manufacturing. The use of plywood makes the fuselage rigid and durable and allows it to handle flight loads and landing forces.

Further attempts to reduce weight were executed by making material cutouts in non-critical areas, basically trimming down some structural dimensions and also supporting areas where stresses are expected to be the highest. From the initial box design, curves were added to the fuselage structure to keep the incoming airflow continuous, effectively improving the aircraft's aerodynamic performance. Quantitatively, we are able to reduce weight by 200 g from material cutouts. Detailed analysis will be made to verify the overall structural integrity.

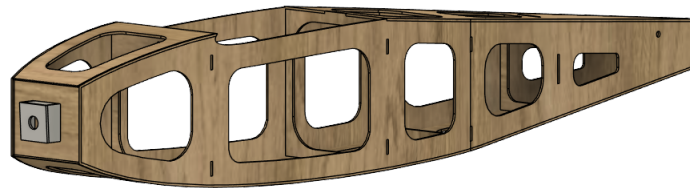


**Figure 5.2:** The CAD skeletal structure of the aircraft fuselage.

### 5.3 Landing Gear Choice

A taildragger configuration was selected for the landing gear design to improve control during the aircraft's missions. This configuration naturally offers a higher angle-of-attack for the wing and tails during takeoffs, providing better lift and significantly reduces the takeoff distance. It also provides greater ground clearance, which is imperative as the operations are done on rough and uneven runways. Better clearance helps protect the propeller from hitting the ground. The fuselage will be vertically displaced better, reducing the possible damage of debris to the drop-off mechanism. Overall, this configuration supports aerodynamic performance and control during ground roll tests.

The aircraft taildragger landing gear will be positioned strategically to ensure ground roll stability, an overall safer takeoff performance. One common design guideline is to place the main wheels where the level ground attitude, the line from the center-of-gravity (CG) to the main wheel's contact point, forms an estimated angle of about  $12^\circ$  to  $15^\circ$  forward from vertical. This geometry prevents nose-over during brakes or rough landings, while it allows the wing and tail to provide lift easily during takeoff. It helps to balance the weight distribution, with about 15-20% weight burden to the tailwheel that is ideal for stable and efficient ground handling. *Equation 5.1* will be used to find the needed landing gear dimensions, keeping the assumed angle in mind.

### 5.4 Package Drop-off Mechanism

The payload flight mission mandates the drop-off of the 64 in<sup>3</sup> volume-based payload [P2] during flight. The package drop-off requires a reliable and secure door mechanism design, guaranteeing that the package is ejected without becoming stuck inside its compartment. In addition, the doors must close properly after drop-off to minimize the drag caused by a non-continuous airflow below the fuselage. The initial concept development has a two-door design with two different mechanisms. The gear-driven mechanism is proposed to control the opening and closing of the doors. Another mechanism employs lever arms to open the doors mechanically during package release. A spring-loaded system will be added to safely eject the package out of the compartment. Further physical testing will be required to determine the most effective, fastest and safest package release, keeping the aerodynamic penalties to a minimum.



**Figure 5.3:** The two proposed mechanisms for two-door opening and closing, gear-driven (left) and lever (right)

## 6. Aerodynamics

### 6.1 Assumptions

To properly define the aerodynamic characteristics of our aircraft, we first analyzed the expected flight atmospheric conditions. The main wing dimensions are set in *Table 6.1*. The standard atmospheric conditions of Mission Bay Park, the flight area, were provided in *Table 1.1*. Assuming a cruise speed of 25 m/s and a mean chord length of 0.2 meters, we estimated a Reynolds number ( $Re$ ) of approximately 340,000 *Appendix B.6.3*. This value reflects the flow regime around the airfoil and helps determine aerodynamic performance. Given that airfoil performance data is more readily available at standard Reynolds numbers, we selected airfoils characterized at  $Re = 500,000$  to ensure a conservative and reliable match for our design. Using data from the XFOIL database, we extracted the relevant lift, drag, and parasite drag coefficients for our calculations and performance modeling.

PARAMETER	VALUE	PARAMETER	VALUE
Planform Area (m <sup>2</sup> )	0.27	Aspect Ratio	6.75
Wing Span (m)	1.35	Taper Ratio	1
Chord (m)	0.2	Sweep	0

**Table 6.1:** Main wing dimensions

### 6.2 Airfoil Selection

To determine the optimal airfoil for our wing design, we conducted a 2D aerodynamic analysis using XFOIL at a Reynolds number of 500,000, based on our expected flight conditions of cruise speed of 25 m/s and chord length of 0.2 m. We evaluated five widely used airfoils—NACA 4412, 4415, 2412, 0012, and Clark-Y—focusing on lift coefficient ( $C_l$ ) and drag coefficient ( $C_d$ ) across a range of angles of attack. As shown in the performance plots, NACA 4412 demonstrated the most favorable characteristics, achieving a maximum  $C_l$  of 1.362 at a stall angle of 13.25°, which is the greatest lift coefficient among competitors. Its minimum drag coefficient,  $C_d$ , is 0.0363, however, most of the airfoils have their drag coefficient around that. Our airfoil selection was decided to be the airfoil that provides the best lift among the other candidates as all of the airfoils' drags are quite identical.

These values indicate strong lift performance, efficient cruise behavior, and smooth stall characteristics. Based on this comprehensive comparison, we selected NACA 4412 as our primary wing airfoil for its superior low-speed aerodynamic efficiency and reliability.

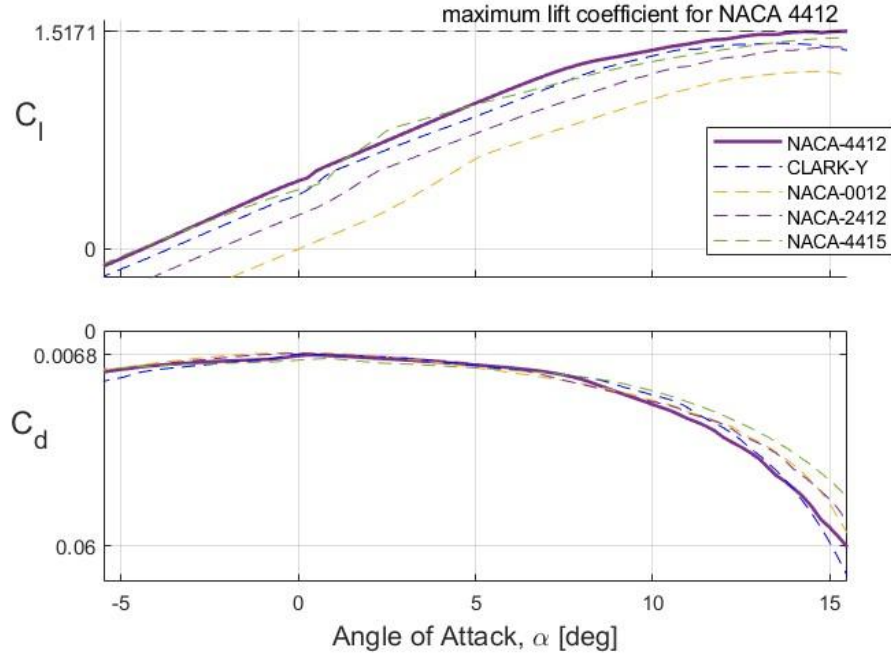


**Figure 6.1:** Selected Airfoils 2-D Aerodynamic Analysis at  $Re = 500,000$  and cruise speed of 25 m/s. Data imported from XFOIL. Lift Coefficient (top) and Drag Coefficient (bottom) vs Angle of Attack. Stall Angle of Attack at  $13.25^\circ$

PARAMETER	VALUE	PARAMETER	VALUE
$CL_{max}$	1.36222	AOA stall	$13.25^\circ$
$CD_{min}$	0.0363	$S_{wet}/S_{ref}$	2.0480
$(L/D)_{max}$	35.838	$K''$	0.01344
$Cl_{min}$	-0.8699	$a_0$	$-4.5^\circ$

**Table 6.2:** Major Aerodynamic Parameters of selected airfoil, NACA 4412.

### 6.3 Drag Buildup

To estimate the total drag of the aircraft, we used the drag build-up method based on Raymer's approach, incorporating skin friction coefficients ( $C_f$ ), form factors (FF), interference factors (Q), and wetted area ratios ( $S_{wet}/S_{ref}$ ) for each major component. Starting from 2D XFOIL data, we derived  $K'' = 0.01344$  and calculated 3D lift and drag coefficients for a more realistic representation *Appendix A.6.1*.

The wing section had a  $C_f$  of 0.0023, FF of 1.0521, and  $S_{wet}/S_{ref}$  of 2.048, resulting in a  $CD_0$  of 0.0054. The fuselage contributed 0.0063, while the motor and landing gear added 0.019 and 0.0057, respectively. Tail drag contributions were assumed small and are pending

refinement. The total parasite drag coefficient ( $CD_0$ ) was estimated at 0.0363, which matches the minimum value on the plotted 3D drag curve. This curve includes the aerodynamic effects of the full aircraft and a more detailed drag buildup for each aircraft part is in *Appendix C.6.1*.

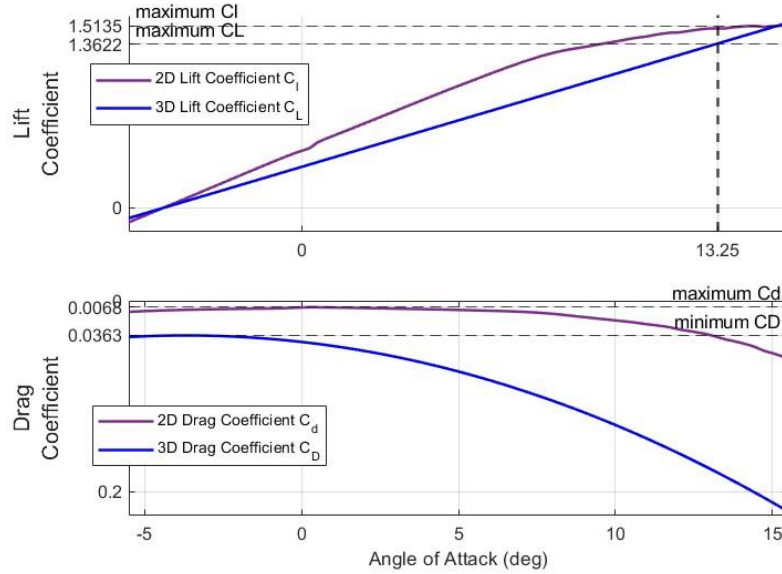


**Figure 6.2:** 2-D and 3-D comparison. Lift coefficient with  $CL_{\max}$  at  $13.25^\circ$  stall angle of attack (top); Drag coefficient vs angle of attack, 3-D includes the drag build-up for wing, fuselage, tails, propeller and landing gear. (bottom)

## 7. Performance

### 7.1 Takeoff

In order to calculate the takeoff distance (SG) and performance of the aircraft equations 7.1-7.4 was implemented in a MATLAB code with the estimated gross weight, wing loading, and wing design parameters from the initial sizing as illustrated in *Figure A.7.1*. Additionally due to rough runway conditions at Mission Bay park the rolling friction coefficient was assumed to be 0.03. This resulted in a takeoff distance of around 12.26 meters with a corresponding stall speed of 9.314 m/s. This gives a rather quick takeoff performance on par with similar RC aircraft in a sport category which would further be improved due to the plane's tail dragger configuration. Furthermore, due to the large runway distance (~80 m) at mission bay as shown in *Figure A.7.2* this plane design provides ample room in case of emergencies or issues at takeoff.

### 7.2 Cruise

Since the goal of this design was to minimize the flight time as much as possible the calculation of thrust versus cruise velocity was utilized to find the total range of values, and the

nominal cruise speed based on the chosen propeller/motor combination. In order to get a more accurate representation of this plot the 3D aerodynamic coefficients and the estimated max gross weight of 2 kg was used. This assumed steady level flight as such lift was set to gross weight and thrust was set to equal drag.

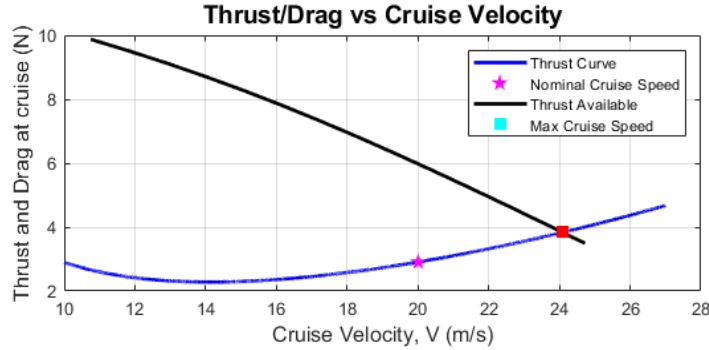


**Figure 7.1:** Thrust required for steady level flight given different cruise velocities.

As illustrated in *Figure 7.1* the thrust required at nominal cruise speed is around 3 newtons and the max cruise speed given propellers available thrust at max power calculated at 3.83 N gives a max cruise speed of 24 m/s.

### 7.3 Maneuvering and Climb

With the designed wing loading, 3D aerodynamic coefficients, 2 kg gross weight, and desired 0.5 thrust to weight ratio it was found that our maximum load factor during maneuvering is that of 4 and the maximum climb angle was that of 15° using *Appendix B.7.5-6* as highlighted in *Figure 7.2*.

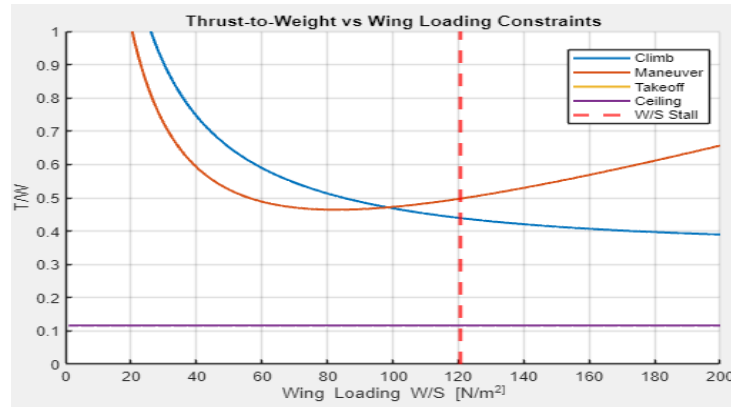


**Figure 7.2:** T/W vs Wing loading at set performance and aerodynamic design parameters.

These two values ensure a very agile and quick performance necessary for the proposed mission segments and target goal of minimizing flight time.

## 8. Propulsion

### 8.1 Propulsion System Design

The propulsion system of the aircraft consists of a Cobra C-2217/16 brushless motor with a given input voltage of 11.1V. We calculated a maximum motor speed to be approximately 13098 RPM. Considering an operating range of 50-80% of this maximum, the usable RPM range becomes roughly 6500 to 10500 RPM. As stated in the performance section, we have determined that the thrust needed to maintain our 20 m/s cruise speed is 3N. With these constraints a propeller analysis was required to determine the correct sizing for our aircraft. Within the target RPM range, we compared various suitable propellers *Appendix C.9.3*. The APC 8x6-E propeller demonstrated the highest efficiency ( $\eta$ ) versus advance ratio (J) in Figure 1, with the APC 9x6-E closely behind. Although the 8x6-E showed superior efficiency, power coefficient (Cp), torque coefficient (Cq), and thrust coefficient (Ct) across *Appendix A.8.1-4*. However, further evaluation, using *Table 8.1*, revealed a critical performance shortfall: the APC 8x6-E fails to meet the required 3 N of thrust at cruise. This level of thrust is only achieved above 9000 RPM, which pushes the motor to operate near the upper limit of the defined range – exceeding our efficiency and reliability constraints. In contrast, The APC 9x6-E delivers a more favorable thrust profile at cruise conditions. At 9000 RPM, it produces approximately 3.75 N of thrust, compared to only 2.66 N from the APC 8x6-E. Given its ability to meet thrust requirements within the acceptable RPM range and its performance at the cruise advance ratio, the APC 9x6-E was selected as the optimal propeller for our aircraft.

Propeller	$\eta_p$	Thrust [N]	Torque [Nm]	Power [W]	J	n [RPM]
<b>9x6E</b>	<b>0.724</b>	<b>3.75</b>	<b>.112</b>	<b>105.29</b>	<b>0.583</b>	<b>9000</b>
<b>8x6E</b>	<b>0.736</b>	<b>2.66</b>	<b>0.077</b>	<b>72.20</b>	<b>0.655</b>	<b>9000</b>

**Table 8.1:** Propulsion Key Parameters comparison between 9x6E and 8x6E.

## 9. Weights and Balances

### 9.1 Weight Breakdown

Using initial sizing estimates, desired payload weight, gross weight, preliminary CAD, and measured mass of plane components resulted in the breakdown of weights as illustrated in pie chart on the left of figure 9.1. From this it was calculated that about  $\frac{1}{3}$  of the total gross weight came solely from payload 1 whilst both the fuselage and wing had about a  $\frac{1}{6}$  of the gross weight each. As a result the estimated empty weight fraction was found to be 0.66. In terms of the structural weight of the plane highlighted by the pie chart to the right of figure 9.1 the plane is  $\frac{2}{3}$  made of wood followed by 3D printed plastic and foam.

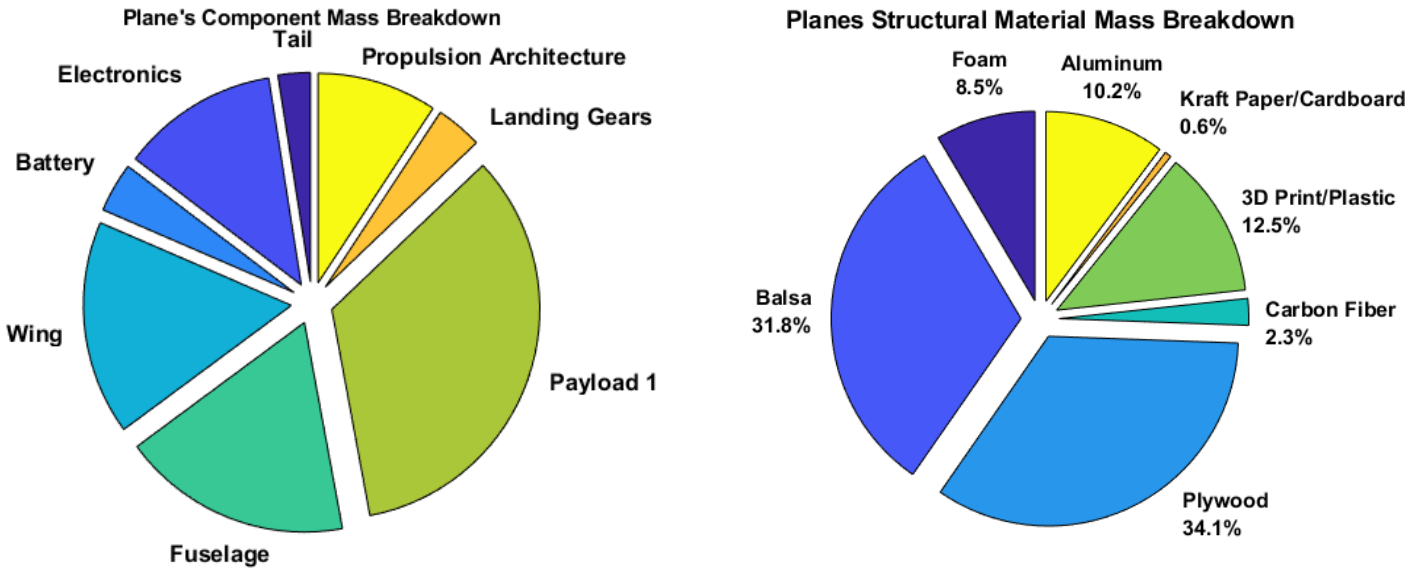


**Figure 9.1:** Breakdown of Aircraft Weight and Material Composition

## 9.2 Tail Sizing

Since the goal of the is a quick flight time with agile maneuvering the tail sizing needed to reflect the adequate control and stability necessary. As such the vertical tail volume coefficients that match a homebuilt from *Figure A.9.2* in the appendix and similar reference RC aircraft sources a  $C_{VT}$  and  $C_{HT}$  of about 0.04 and 0.35 respectively was chosen for adequate control. To further minimize drag and structural weight an aspect ratio of 4 and 2 for horizontal and vertical tail was chosen with the moment arm distance (i.e. distance from wing quarter-chord to tail quarter-chord) for both tails set to 0.42 m. With the volume coefficients, moment arms, wing area, and wing span the tail area was calculated using *Appendix B.9.1* [1] producing the results in *Table 9.1*. To achieve great stability, agility, and sufficient tail authority both vertical and horizontal tails utilized a NACA 0012 airfoil due its ability to satisfy the aforementioned characteristics in addition to its proven reliability and symmetric shape for aerobatic maneuvers.

PLANFORM AREA	VALUE
Vertical Stabilizer ( $S_{VT}$ )	0.0347 m <sup>2</sup>
Horizontal Stabilizer ( $S_{HT}$ )	0.045 m <sup>2</sup>

**Table 9.1:** Tail Sizing Dimensions

## 9.3 Stability

To achieve stability in flight the initial goal was to place the plane's center of gravity at the quarter chord in all 3 flight configurations (empty, takeoff, dropoff). This led to the

placement of individual masses/components detailed in *Table 9.1* along for which was inputted to *Appendix B.9.3* to find the overall CG location with the reference point being the nose of the fuselage structure. As such this resulted in the CG locations found in *Table 9.2* in which all three configurations are slightly forward of the wing quarter-chord location providing ample self correcting stability during flight in case of strong wind gusts which is typical in coastal regions like Mission Bay Park. In addition to CG location the neutral point and static margin were calculated using inputs from *Appendix C.9.2* into *Appendix B.9.3-5* resulting in a static margin range from 16.52-17.32 % from the mean aerodynamic chord. With this range of static margin the plane is set to be more than adequately stable ensuring safe and maneuverable flights in most conditions particularly coastal wind gusts.

<b>Stability Parameters Results</b>	<b>Percentage (%) from MAC</b>
Center of Gravity (Empty Flight)	24.73
Center of Gravity (w/ Payloads 1 & 2 )	24.05
Center of Gravity (w/ Payloads 1)	23.97
Neutral Point	41.27
Static Margin(Empty Flight )	16.52
Static Margin(w/ Payloads 1 & 2 )	17.22
Static Margin(w/ Payloads 1 )	17.32

**Table 9.2:** Aerodynamic stability results

## 10. Conclusion

The Jark MK.II was developed with the primary goal of maximizing payload-based profit while maintaining aerodynamic efficiency, structural simplicity, and operational reliability. Through a data-driven scoring function and careful trade-off analyses, our team prioritized carrying the heavier package while still accommodating a volume-based payload. The final configuration features a high-wing design with 3° dihedral for roll stability, a balsa rib-and-spar wing for lightweight strength, and a semi-monocoque plywood fuselage optimized for internal volume and manufacturability. A taildragger landing gear setup was selected to improve takeoff performance and increase ground clearance, especially for mid-flight payload drops. Aerodynamic efficiency was validated through 2D and 3D airfoil analyses, confirming the NACA 4412 as the optimal choice. A drag build-up approach yielded a total parasite drag coefficient of 0.0363, guiding cruise and propulsion sizing. Propulsion analysis led to the selection of the APC 9x6-E propeller, capable of delivering the required thrust within efficient RPM ranges. With proven structural stability, balanced weight distribution, and strong aerodynamic performance, the Jark MK.II is well-positioned to meet its dual-payload delivery mission successfully.

## References

- [1] - Raymer, Daniel P. *Aircraft Design: A Conceptual Approach: A Conceptual Approach*. 6th ed., American Institute of Aeronautics and Astronautics Inc, 2018.
- [2] - *NACA 4412 (NACA4412-IL) Xfoil Prediction Polar at Re=1,000,000 Ncrit=5*, [airfoiltools.com/polar/details?polar=xf-naca4412-il-1000000-n5](http://airfoiltools.com/polar/details?polar=xf-naca4412-il-1000000-n5). Accessed 19 Mar. 2025.
- [3] - Hwang, J.T, MAE 155B Lectures, University of California San Diego
- [4] - Hwang, J.T, MAE 155A Lectures, University of California San Diego
- [5] - <https://www.apcprop.com/technical-information/performance-data/>
- [6] - <https://www.cobramotorusa.com/motors-2217-16.html>

# Appendices

## Appendix A - Figures

### A.5

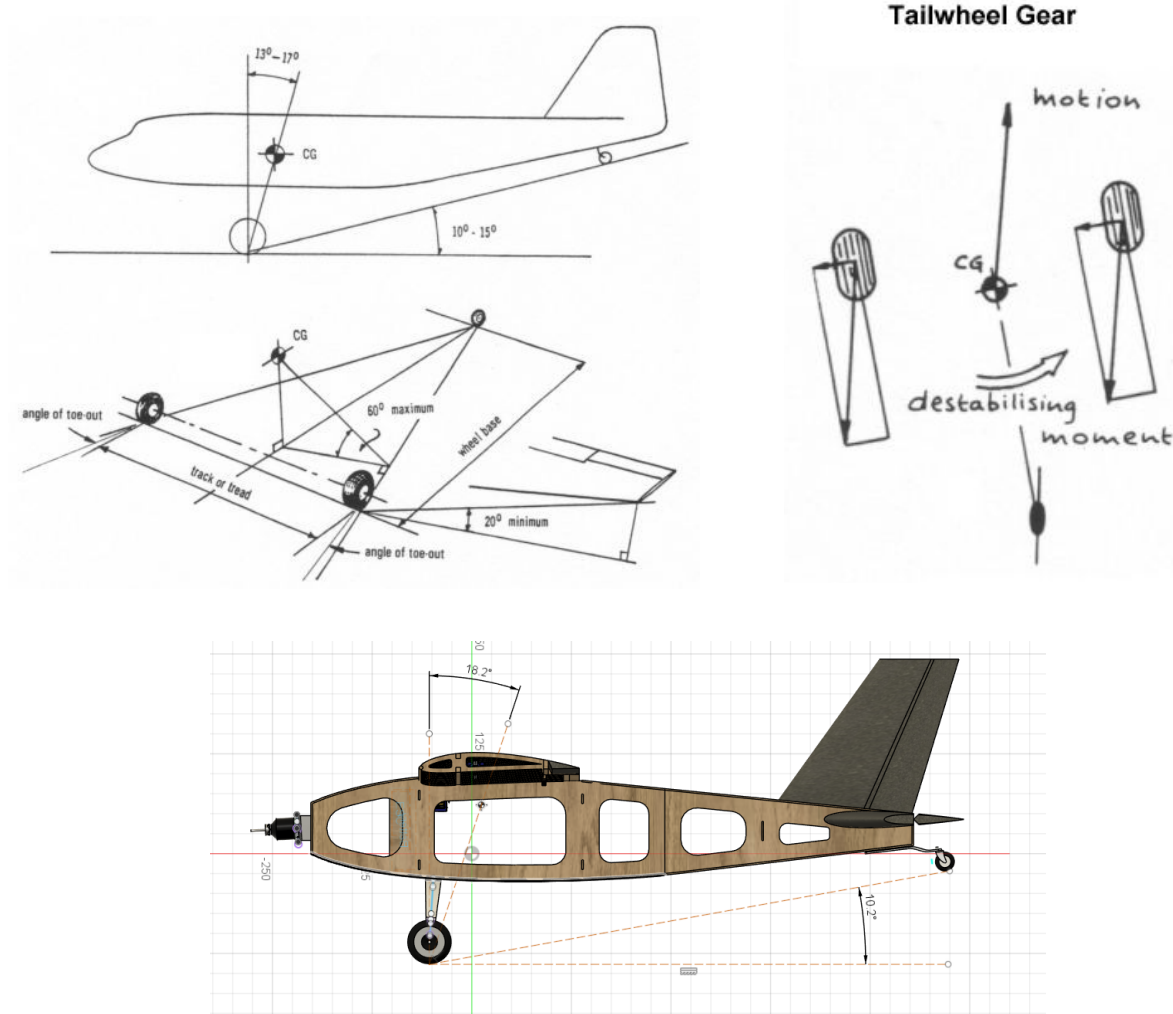


**Figure A.5.1:** The landing gear configuration (Tail dragger).

## A.6

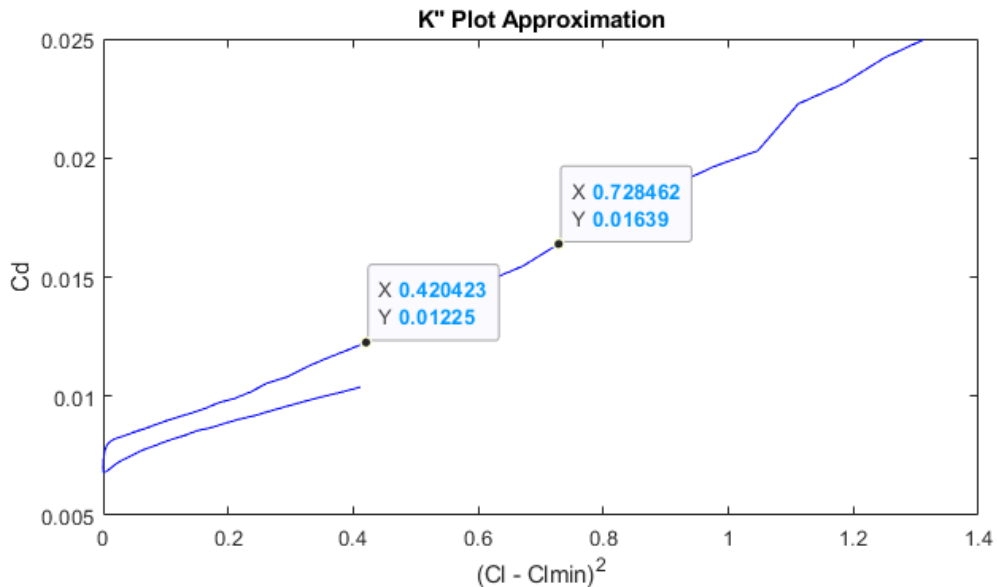


**Figure A.6.1:** K'' estimation from the 2-D aerodynamic data for 3-D aerodynamic data calculations in Figure 6.2.

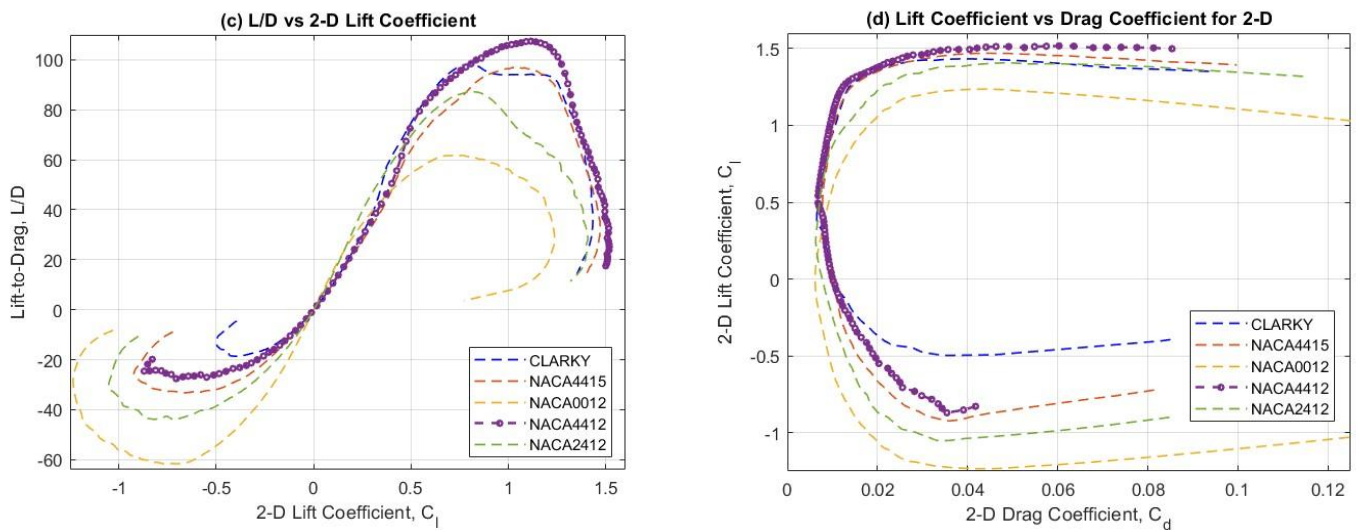


**Figure A.6.2:** Other 2-D aerodynamic data for selected airfoils at  $Re = 500,000$ . Data collected from XFOIL.

## A.7

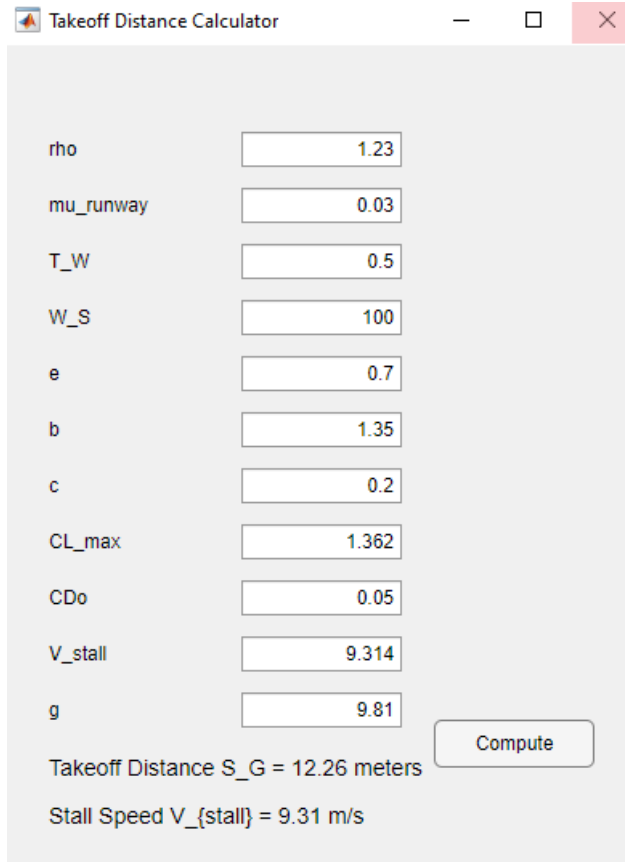


**Figure A.7.1:** The Graphical User Interface (GUI) of takeoff distance and stall speed calculations using MATLAB.



**Figure A.7.2:** Top View of Mission Bay Runway with approximate total runway distance (80m) using ArduPilot Mission Planner Software.

## A.8

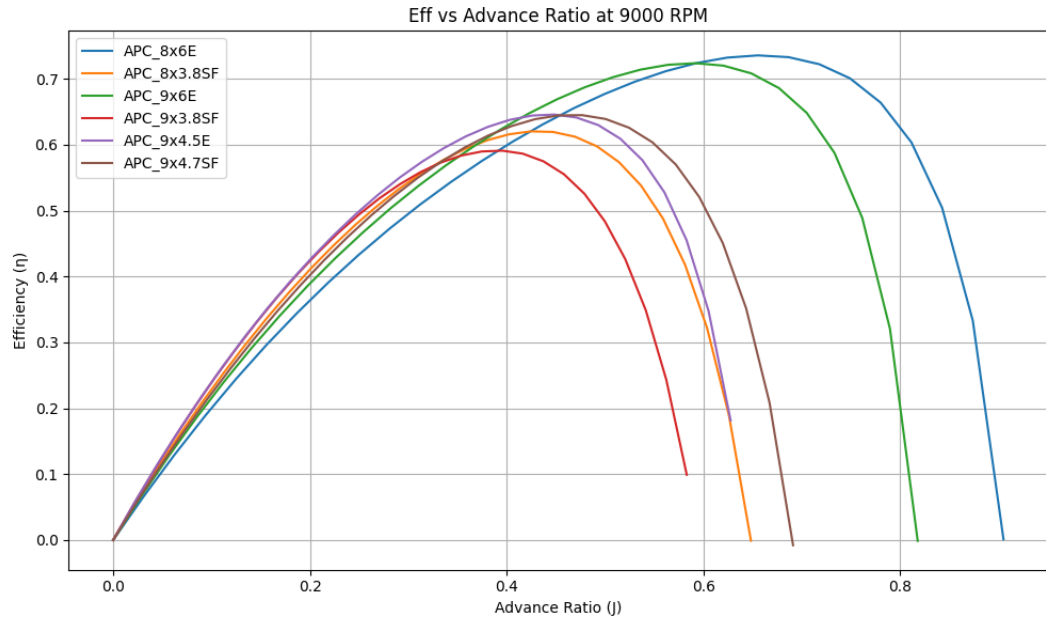


**Figure A.8.1:** Efficiency of different propellers as a function of advance ratio.

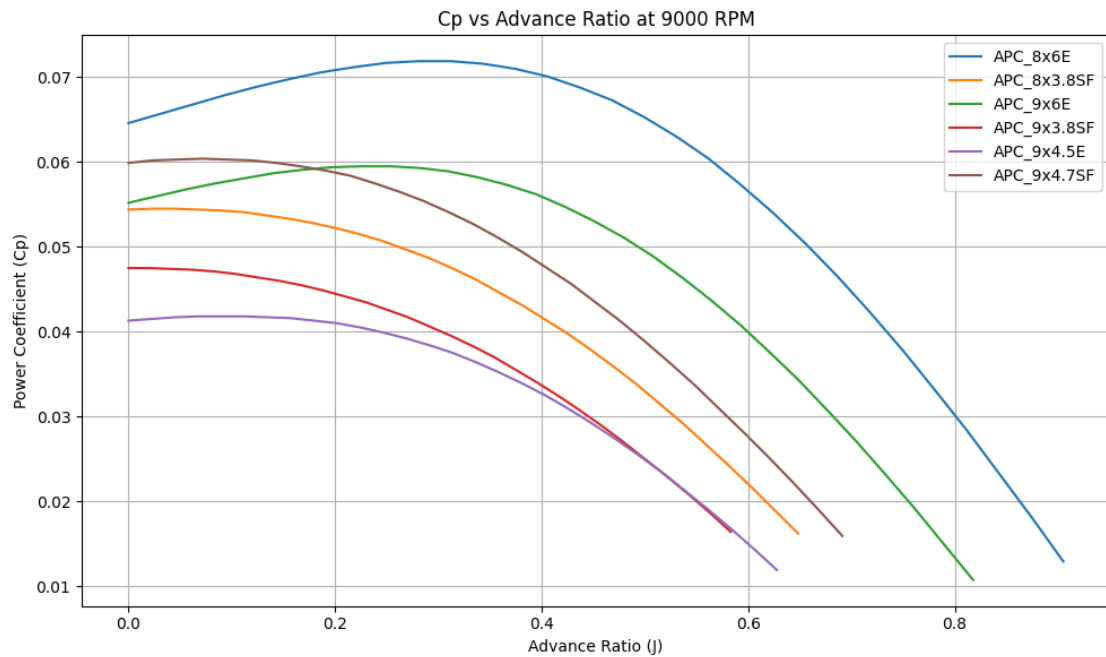
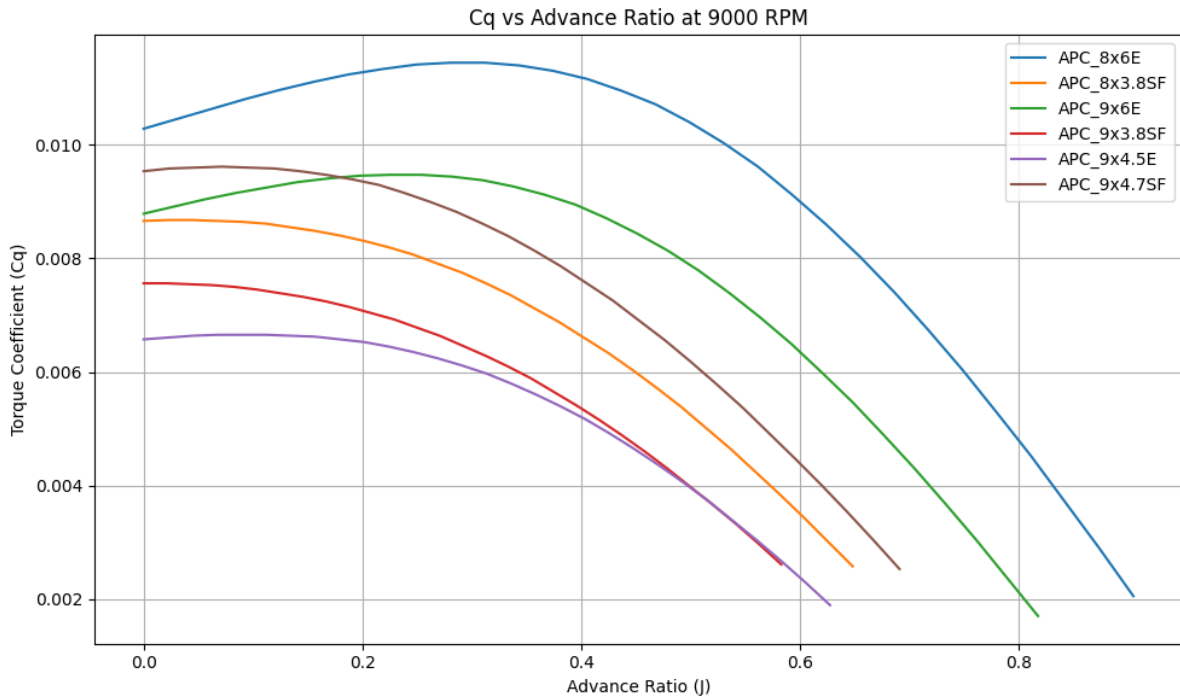
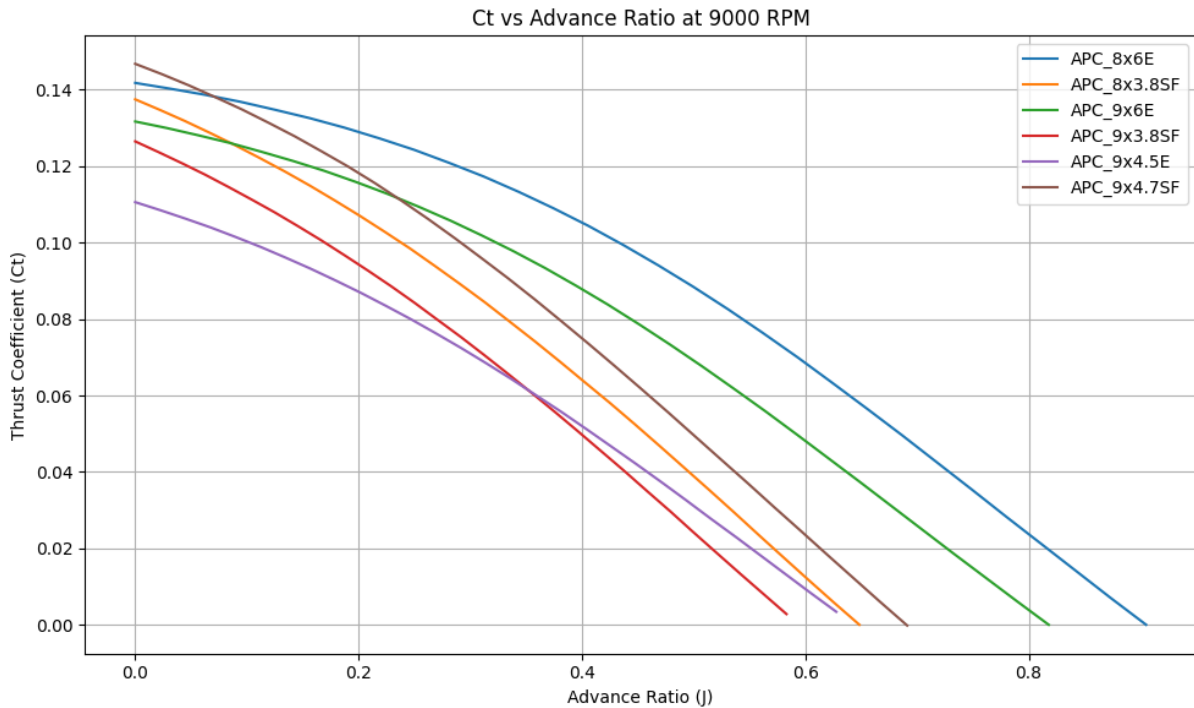


Figure A.8.2: Power coefficient of different propellers as a function of advance ratio.



**Figure A.8.2:** Torque coefficient of different propellers as a function of advance ratio.



**Figure A.8.3:** Thrust coefficient of different propellers as a function of advance ratio.

## A.9

	Typical values	
	Horizontal $c_{HT}$	Vertical $c_{VT}$
Sailplane	0.50	0.02
Homebuilt	0.50	0.04
General aviation—single engine	0.70	0.04
General aviation—twin engine	0.80	0.07
Agricultural	0.50	0.04
Twin turboprop	0.90	0.08
Flying boat	0.70	0.06
Jet trainer	0.70	0.06
Jet fighter	0.40	0.07–0.12*
Military cargo/bomber	1.00	0.08
Jet transport	1.00	0.09

Figure A.9.1: Image of table 6.4 from Raymer [1] textbook that lists typical Tail Volume Coefficients

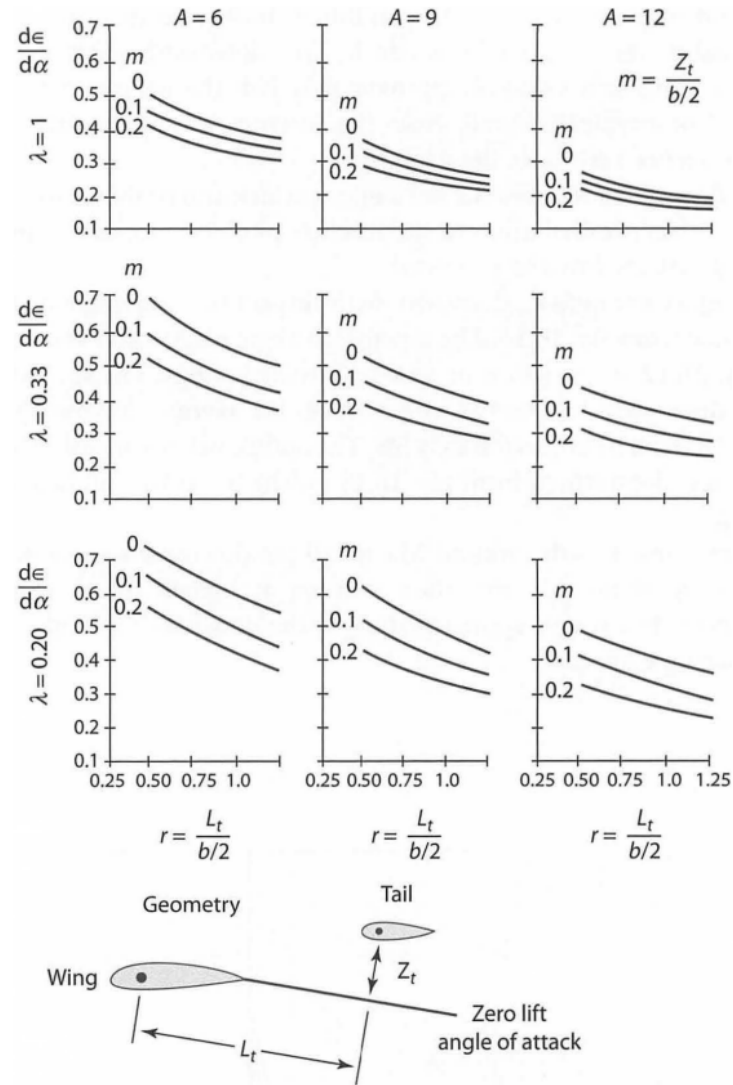


**Figure A.9.2:** Plots of different  $\frac{d\epsilon}{d\alpha}$  vs  $r$  coefficient at varying taper,  $m$  coefficient, and aspect ratio.

## Appendix B - Equations

### B.4

**B.4.1:** Gross Weight Equation:

$$W_g = W_p + W_e + W_b$$

**B.4.2:** Scoring Function Equation

$$J(x) = \frac{r_{wp} W_p(x) + r_{vp} V_p(x) - c_e E_f(x) - c_c}{T_f(x)} - \frac{c_{wg} W_g(x)}{t_l} - c_f$$

### B.5

**B.5.1:** Taildragger Landing Gear Equation

$$d_{forward} = h_{CG} x \tan(\theta)$$

### B.6

**B.6.1:** Total Drag Coefficient Equation

$$C_D = C_{D,0} + \frac{C_L^2}{\pi \cdot e \cdot AR}$$

**B.6.2:** Drag Buildup — form and interference drag Equation

$$C_{D,0} = \frac{\sum (C_{fi} FF_i Q_i S_{wet_i})}{S_{ref}}$$

**B.6.3:** Reynolds Number Equation

$$Re = \frac{\rho V_{cruise} C}{\mu}$$

**B.6.4:** 3-D Maximum Lift Coefficient Equation

$$C_{L,max} = 0.9 C_{l,max} \cos(\Lambda_{c/4})$$

## B.7

**B.7.1-4:** Aircraft Takeoff Distance Equations

$$\begin{aligned} K &= \frac{1}{\pi e A R} \\ K_T &= \left( \frac{T}{W} \right) - \mu \\ K_A &= \frac{\rho}{2(W/S)} (\mu C_L - C_{D,0} - KC_L^2) \\ S_G &= \left( \frac{1}{2gK_A} \right) \ln \left( \frac{K_T + K_A V_f^2}{K_T + K_A V_i^2} \right) \end{aligned}$$

**B.7.5-6:** Climb and Maneuvering Thrust to Weight Equations

$$\begin{aligned} \frac{T}{W} &\geq \sin(\gamma) + \frac{W/S}{\pi e A R q} + \frac{C_{D,0} q}{W/S} \\ \frac{T}{W} &\geq n^2 \frac{W/S}{\pi e A R q} + \frac{C_{D,0} q}{W/S} \end{aligned}$$

## B.8

**B.8.2:** Aileron Area Equation

$$\text{Aileron Area} = \text{Aileron Chord} \times \text{Aileron Span}$$

**B.8.2:** Elevon Area Equation

$$\text{Elevon Area} = \text{Elevon Chord} \times \text{Elevon Span}$$

## B.9

**B.9.1:** Horizontal and Vertical Tail Planform Area Equation

$$\begin{aligned} S_{HT} &= \frac{c_{HT} C_W S_W}{L_{HT}} \\ S_{VT} &= \frac{c_{VT} b_W S_W}{L_{VT}} \end{aligned}$$

**B.9.2:** Center of Gravity Location Equation

$$x_{cg} = \frac{\sum_i W_i x_{cg,i}}{\sum_i W_i}$$

**B.9.3:** Horizontal Tail Lift Curve slope Equation

$$\frac{dC_{L,t}}{d\alpha} = \frac{dC_{L,t}}{d\alpha.t} \left(1 - \frac{d\varepsilon}{d\alpha}\right) \eta_h$$

**B.9.4:** Neutral Point Location formula

$$x_{np} = \frac{\sum_i \frac{dC_{L,i}}{d\alpha} S_i x_{ac,i}}{\sum_i \frac{dC_{L,i}}{d\alpha} S_i}$$

**B.9.5:** Static Margin Equation

$$SM = \frac{x_{np} - x_{cg}}{mac}$$

## Appendix C - Tables

### C.4

Revenue per unit payload weight	$r_{W_p}$	1
Revenue per unit payload volume	$r_{V_p}$	300
Cost per unit energy	$c_e$	0.3
(COC) Cost per flight	$c_c$	0.5
Cost per unit gross volume	$c_{W_g}$	300
(COF) Cost per unit flight-time	$c_f$	0.2
Total flight time in aircraft life	$t_l$	1000

**Table C.4.1:** Scoring Function's fixed parameter values

Gravitational Acceleration	$g$	9.81 [m/s <sup>2</sup> ]	Given (Earth's Gravity)
Battery Parameters	$n_b$	0.85	Assumption
	$e_b$	453069.786	= (11.1 v)(1.8 Ah)(3600 J/Wh)/(0.158757 kg)
Flight Range	$R_{\text{flight}}$	600 [m]	Provided in <i>Table 1.1</i>
Lift-to-Drag Ratio	$L/D$	8-13	Assumption
	$Tf(x)$	—	= 20*R_flight / 3600*V_cruise
Require Thrust to maintain cruise	Thrust_req_cruise	—	= 4.4482216153 * (1 / (L/D)) * W_g
Power	$P_{\text{in}}$	—	= Thrust_req_cruise*V_cruise/1000
	$E_f(x)$	—	= (20*P_in/n_b) * (R_flight/3600*V_cruise)
Known Weight	$W_{\text{known}}$	0.8642 [lb]	Given (Component Weights)
Airframe Weight	$W_{\text{airframe}}$	2.0358 [lb]	= W_g - W_known - Wp(x)
Empty Weight	$W_e$	2.9 [lb]	= W_known + W_airframe
	$W_e/W_g$	0.66	= W_e/W_g
Gross Weight	$W_g$	4.4 [lb]	Assumption
Cruise Speed	$V_{\text{cruise}}$	25 [m/s]	Assumption
Payload Weight	$W_p$	1.5 [lb]	Assumption

**Table C.4.2:** Scoring Function's Parameter Assumptions and Values

**From the student-built aircrafts' reference sizing values:**

Wing Loading	W/S	100 N/m <sup>2</sup>
Thrust-to-weight	T/W	0.8

**Utilized to make initial assumptions for:**

Gross Weight	$W_g$	4.4 lb
Wing Area	A	0.27 m <sup>2</sup>

**Table C.4.3:** Assumptions on initial gross weight and wing area based on student-built aircrafts (MAE 155B)

## C.5

**FIXED COMPONENT**

<b>Transmitters</b>	RotorLogic RadioMaster TX16S
<b>Batteries</b>	Tattu 11.1V 1800mAh 3S 45C LiPo
<b>Motor</b>	Cobra C-2217/16 Brushless, Kv=1180 <sup>1</sup>
<b>Speed controller</b>	40 Amp ESC <sup>2</sup>
<b>Receivers</b>	FrSky Taranis Receiver X8R 8 Channel
<b>Servos</b>	Smraza 10 Pcs SG90 9G Micro Servo
<b>Servo extensions</b>	30 Pcs 3-Pin Extension Cable
<b>Servo linkages</b>	Pushrod, 16.5" <sup>3</sup> Linkage stoppers <sup>4</sup> Control horns <sup>5</sup>
<b>Some battery monitor</b>	Treat like another battery in size/volume
<b>Landing gear</b>	Aluminum landing gear set—Cessna 182 Parts

Table C.5.1: List of the fixed components and available components

**MATERIALS & DESCRIPTIONS**

<b>Wing spar</b>	Flat carbon fiber, 1 x 6 x 1000 mm Circular tube, 0.32"/0.25" outer/inner diameter, 60" long <sup>6</sup>
<b>Epoxy glue</b>	BSI-201 Quik-Cure Epoxy
<b>Rubber bands</b>	—
<b>Nuts / bolts</b>	M5 x 6mm/8mm/10mm
<b>Tail boom</b>	Circular tube, 0.715"/0.625" outer/ inner diameter, 70" long <sup>7</sup>
<b>Foam boards</b>	— <sup>8</sup>
<b>Balsa sheets</b>	1/16" thick, 8" x 12"
<b>Balsa sticks</b>	Square section, 1/8", 12" long
<b>Fasteners</b>	Cable straps and cable ties

Table C.5.2: List of the available parts and materials

<sup>1</sup> [Cobra C-2217/16 Brushless Motor, Kv=1180](#)<sup>2</sup> [Amazon.com: Flycolor 40A ESC 2-4S Electric Speed Controller 5v 3A BEC with XT60 & 3.5mm Bullet Plugs for RC Drone Airplane Brushless Motors : Toys & Games](#)<sup>3</sup> [16.5" Push Rods \(8-Pack\) | RC Plane Building Materials | Flite Test](#)<sup>4</sup> [Quick-Connect Linkage Stoppers \(6-Pack\) | RC Plane Building Materials | Flite Test](#)<sup>5</sup> [FT Control Horn \(20 pieces\) | RC Plane Building Materials | Flite Test](#)<sup>6</sup> [Carbon Fiber Roll Wrapped Tube, 0.320"OD](#)<sup>7</sup> [Carbon Fiber Roll Wrapped Tube, 0.711"OD](#)<sup>8</sup> [Elite Test Retail Store - Not Found](#)

## MATERIALS & DESCRIPTIONS

<b>Velcro</b>	16' long, 0.75" wide strips
<b>Hinges</b>	11x25.5 mm 0.43" x1.0"
<b>Hardwood blocks</b>	1"~4" blocks, maple, cherry, walnut
<b>Plywood</b>	1/8" x 12" x 24" birch plywood
<b>Basswood</b>	1/16" x 12" x 8" basswood sheets
<b>Foam</b>	2" x 4' x 8' 25 PSI blue foam
<b>Monokote</b>	White, yellow, blue
<b>Sandpaper</b>	—
<b>Duct tape</b>	—
<b>Vinyl/plastic gloves</b>	—
<b>GPS speed tracker</b>	SKYRC GSM-015

**Table C.5.3:** List of the other available parts and materials

## PROPELLER

<b>b9x6sf<sup>9</sup></b>	<b>11x8e<sup>10</sup></b>
<b>b9x9e<sup>11</sup></b>	<b>b12x6e<sup>12</sup></b>
<b>b9x7-5e<sup>13</sup></b>	<b>b12x8e<sup>14</sup></b>
<b>10x7e<sup>15</sup></b>	<b>13x8e<sup>16</sup></b>
<b>10x10e<sup>17</sup></b>	<b>13x6-5e<sup>18</sup></b>

**Table C.5.4:** List of the propeller choices

## C.6

Part	Cf	FF	Q	Swet/Sref	C <sub>D0</sub> (Raymer)
Wing Section	0.0023	1.0521	1.1	2.047957	0.0054
Fuselage	0.0023	1.2347	1.1	From code	0.0063
Landing Gear	0.0023		1.1	From code	0.0057
Motor	0.0023		1.1	From code	0.019
		<b>Total</b>			<b>0.0364</b>

**Table C.6.1:** Drag buildup for the 3D drag aerodynamic analysis

<sup>9</sup> [B9x6SF - APC Propellers](#)

<sup>10</sup> [11x8E - APC Propellers](#)

<sup>11</sup> [B9x9E - APC Propellers](#)

<sup>12</sup> [b12x6E - APC Propellers](#)

<sup>13</sup> [B9x7.5E - APC Propellers](#)

<sup>14</sup> [b12x8E - APC Propellers](#)

<sup>15</sup> [10x7E - APC Propellers](#)

<sup>16</sup> [13x8E - APC Propellers](#)

<sup>17</sup> [10x10E - APC Propellers](#)

<sup>18</sup> [13x6.5E - APC Propellers](#)

## C.8

<b>SPECIFICATIONS</b>		<b>BRUSHLESS MOTOR Cobra C-2217/16</b>
<b>Weight [kg]</b>		73.0 grams
<b>Size [mm]</b>		mm (diameter) x mm (thickness)
<b>Max Power [W]</b>		265 Watts
<b>Max Thrust [kg]</b>		—
<b>Max Amp [A]</b>		24 Amps
<b>KV rating</b>		1180
<b>ESC</b>		—

**Table C.8.1:** Specifications of the required brushless motor.<sup>19</sup>

<b>SPECIFICATIONS</b>	<b>BATTERY [Tattu]</b>
<b>Weight [kg]</b>	158g
<b>Size [mm]</b>	106*35.5*21mm Tattu 11.1V 1800mAh 3S 45C LiPo Battery Pack
<b>Voltage [V]</b>	11.1 Volts
<b>Energy density</b>	200Wh/kg energy density

**Table C.8.2:** Specifications of the required battery<sup>20</sup>.

<sup>19</sup> [Cobra C-2217/16 Brushless Motor, Kv=1180](#)

<sup>20</sup> [Amazon.com: Tattu 11.1V 1800mAh 3S 45C LiPo Battery Pack with XT60 Plug for Skylark M4-FPV250 Mini Shredder 200 INDY250 PLUS MOJO 280 QAV250 Vortex Emax Nighthawk 250 RC Heli Airplane UAV Drone FPV : Toys & Games](#)

FIXED COMPONENT	BATTERY Tattu
Transmitters	RotorLogic RadioMaster TX16S
Batteries	Tattu 11.1V 1800mAh 3S 45C LiPo
Motor	Cobra C-2217/16 Brushless, Kv=1180 <sup>21</sup>
Speed controller	40 Amp ESC <sup>22</sup>
Receivers	FrSky Taranis Receiver X8R 8 Channel
Servos	Smraza 10 Pcs SG90 9G Micro Servo
Servo extensions	30 Pcs 3-Pin Extension Cable
Servo linkages	Pushrod, 16.5" <sup>23</sup> Linkage stoppers <sup>24</sup> Control horns <sup>25</sup>
Landing gear	Aluminum landing gear set—Cessna 182 Parts Replacement 40 Size ARF PNP

Table C.8.3: List of the fixed components and available components

PROP SIZE	PROP RPM
APC 8x3.8-SF	10,250
APC 8x6-E	9,790
APC 9x3.8-SF	9,560
APC 9x6-E	9,450
APC 9x4.5-E	9,860
APC 9x4.7-SF	9,684

Table C.8.4: List of the propeller size choices and corresponding RPMs.

<sup>21</sup> [Cobra C-2217/16 Brushless Motor, Kv=1180](#)

<sup>22</sup> [Amazon.com: Flycolor 40A ESC 2-4S Electric Speed Controller 5v 3A BEC with XT60 & 3.5mm Bullet Plugs for RC Drone Airplane Brushless Motors : Toys & Games](#)

<sup>23</sup> [16.5" Push Rods \(8-Pack\) | RC Plane Building Materials | Flite Test](#)

<sup>24</sup> [Quick-Connect Linkage Stoppers \(6-Pack\) | RC Plane Building Materials | Flite Test](#)

<sup>25</sup> [FT Control Horn \(20 pieces\) | RC Plane Building Materials | Flite Test](#)

## C.9

Component Name	X <sub>CG</sub> (m) distance from Fuselage Nose	Mass (g)
APC 9x6E Propeller	-0.05	18.8
Cobra 2217/16 Motor	-0.03	76.3
Nose Cone	-0.03	90.9
Electronics Box	0.05	320
Front Landing Gear	0.15	54.1
Payload 1	0.175	681
Wing	0.18	330
Payload 2	0.24	5
Tail Control Surface Servos	0.29	20
Fuselage Structure	0.33	336
Tail Structure	0.6	50
Rear Landing Gear	0.64	17.9
<b>Total</b>		<b>2000</b>

**Table C.9.1:** List of individual component's mass and center of gravity location from fuselage structure nose along X axis; electronics box includes battery, receiver, ESC, Watt meter and balsa wood structure

PARAMETERS	VALUE
Wing Lift Curve Slope ( $\frac{dC_{L,W}}{d\alpha}$ )	6.0752 rad <sup>-1</sup>
Tail Lift Curve Slope ( $\frac{dC_{L,T}}{d\alpha_T}$ )	6.3 rad <sup>-1</sup>
Downwash-Angle Derivative ( $\frac{d\varepsilon}{d\alpha}$ )	0.46
Tail Efficiency Factor ( $\eta_h$ ) [3]	0.9
Tail Lift Curve Slope ( $\frac{dC_{L,T}}{d\alpha}$ )	3.0618 rad <sup>-1</sup>

**Table C.9.2:** Aerodynamic parameters used to calculate Neutral point

Cobra C2217/16 Motor Propeller Data									
Motor Wind 16-Turn Delta		Motor Kv 1180 RPM/Volt		No-Load Current $I_0 = 0.75$ Amps @ 8V		Motor Resistance $R_m = 0.070$ Ohms		I Max 24 Amps	P Max (3S) 265 W
Prop Manf.	Prop Size	Input Voltage	Motor Amps	Watts Input	Prop RPM	Pitch Speed	Thrust Grams	Thrust Ounces	Thrust Eff. Grams/W
APC	8x3.8-SF	11.1	13.75	152.6	10,250	36.8	839	29.59	5.50
APC	8x4-E	11.1	11.59	128.6	10,610	40.2	719	25.36	5.59
APC	8x6-E	11.1	16.70	185.4	9,790	55.6	832	29.35	4.49
APC	8x6-SF	11.1	21.16	234.9	9,000	51.1	872	30.76	3.71
APC	8x8-E	11.1	21.15	234.8	9,010	68.3	728	25.68	3.10
APC	9x3.8-SF	11.1	17.78	197.4	9,560	34.4	1068	37.67	5.41
APC	9x4.5-E	11.1	16.10	178.7	9,860	42.0	998	35.20	5.58
APC	9x4.7-SF	11.1	17.07	189.5	9,684	43.1	1050	37.04	5.54
APC	9x6-E	11.1	18.63	206.8	9,450	53.7	1058	37.32	5.12
APC	9x6-SF	11.1	26.94	299.0	7,930	45.1	1081	38.13	3.61
APC	9x7.5-E	11.1	23.84	264.6	8,560	60.8	1036	36.54	3.91
APC	10x3.8-SF	11.1	25.08	278.4	8,250	29.7	1314	46.35	4.72
APC	10x5-E	11.1	21.11	234.3	9,000	42.6	1166	41.13	4.98
APC	10x6-E	11.1	22.19	246.3	8,770	49.8	1224	43.17	4.97
APC	10x7-E	11.1	24.67	273.8	8,320	55.2	1217	42.93	4.44
APC	11x5.5-E	11.1	25.89	287.4	8,114	42.3	1383	48.78	4.81
GWS	8x4-DD	11.1	9.14	101.5	11,020	41.7	656	23.14	6.47
GWS	9x5-DD	11.1	15.60	173.2	9,920	47.0	994	35.06	5.74
GWS	9x5x3-DD	11.1	19.39	215.2	9,330	44.2	1096	38.66	5.09
GWS	10x6-DD	11.1	20.11	223.2	9,190	52.2	1162	40.99	5.21
GWS	10x6x3-DD	11.1	24.39	270.7	8,400	47.7	1322	46.63	4.88

Table C.9.3: List of various off shelf propellers for Cobra C2217 motor at set 11.1 input voltage.

[5]

